

GEOCHEMISTRY

Worm tubes as conduits for the electrogenic microbial grid in marine sediments

Robert C. Aller*, Josephine Y. Aller, Qingzhi Zhu, Christina Heilbrun, Isaac Klingensmith, Aleya Kaushik†

Electrogenic cable bacteria can couple spatially separated redox reaction zones in marine sediments using multicellular filaments as electron conductors. Reported as generally absent from disturbed sediments, we have found subsurface cable aggregations associated with tubes of the parchment worm *Chaetopterus variopedatus* in otherwise intensely bioturbated deposits. Cable bacteria tap into tubes, which act as oxygenated conduits, creating a three-dimensional conducting network extending decimeters into sulfidic deposits. By elevating pH, promoting Mn, Fe-oxide precipitation in tube linings, and depleting S around tubes, they enhance tube preservation and favorable biogeochemical conditions within the tube. The presence of disseminated filaments a few cells in length away from oxygenated interfaces and the reported ability of cable bacteria to use a range of redox reaction couples suggest that these microbes are ubiquitous facultative opportunists and that long filaments are an end-member morphological adaptation to relatively stable redox domains.

INTRODUCTION

Since their discovery in laboratory-incubated sediment (1), cable bacteria, all of which belong to the deltaproteobacterial family Desulfobulbaceae, have been the subject of intense study because of their unique adaptations and nontraditional utilization of redox conditions in sedimentary deposits (2). They are now recognized as being widely distributed in natural systems but under apparently restricted environmental conditions (3–6). The primary conceptual and quantitative model characterization of these organisms is as multicellular filaments extending uninterrupted over centimeter scales from the oxygenated sediment–water interface vertically into underlying sulfidic regions (2, 7). In this mode, filaments act as organically insulated electron conductors directly connecting cathodic reduction in the oxic zone with anodic oxidation in the sulfidic zone, bypassing possible intermediate suboxic zones. Conductive sediment pore water completes the circuit. As a distinctive signature of cable bacteria activity, reduction of O₂ elevates pH and the oxidation of sulfide (HS[−], Fe-sulfides) lowers pH in spatially separated regions, promoting alkalinity production and carbonate and oxide mineral precipitation in the oxic zone, and acid production and carbonate mineral dissolution in a distal sulfidic zone. Additional biogeochemical consequences attributed to cable bacteria are enhancement of sedimentary capture of P and possible modulation of eutrophication dynamics in coastal environments (5, 8).

The uniqueness of cable bacteria has stimulated continued research into their physiology and impacts, with recent observations contributing to a rapidly changing view of this microbial group and the conceptual paradigms surrounding them. It is now known that cable bacteria can use a wide range of cathodic potentials, extending to ~170 mV relative to the standard hydrogen electrode, implying, but not proving, that cathodic reactions coupled to NO₃[−], Mn⁴⁺, and Fe³⁺ can all be used in addition to O₂ (9, 10). A range of reductants can also be used, including dissolved organic matter (e.g., propionate) (11). Rather than

a standalone species, cable bacteria appear to be one component of complex e-community consortia and are apparently heterotrophs closely associated with sulfur-oxidizing chemoautotrophs (11, 12). Their taxonomy may be more diverse than originally recognized, although this is a subject of ongoing research (Supplementary Materials) (10, 13). All of these modifications from the original model imply that cable bacteria consist of multiple species and strains that are metabolically and ecologically flexible. While shown to be ubiquitously distributed, they are believed to be largely inhibited in bioturbated deposits (3, 4, 6). Here, we demonstrate that well-developed filaments can be abundant in stable subdomains of the bioturbated zone of sedimentary deposits, and conclude that the assumed model of cable bacteria likely represents an end member in a metabolic and morphologic continuum for a highly facultative group of microorganisms.

RESULTS

Sampling locations

To examine the possible distributions of cable bacteria in natural bioturbated deposits, we collected box cores from muds in Great Peconic Bay (GPB) during 2016–2018, within the Peconic Estuary System, Long Island, New York, USA. Diver deployed, acrylic corers (30 cm by 30 cm by 10 cm; length, height, width) sampled overlying water and penetrated sediment to ~20 to 25 cm. The site (40°56′055″N and 72°29′877″W) is located at a water depth of ~8 m and has average weight % organic C of ~2.1% and N of ~0.2%, a ²¹⁰Pb accumulation rate of 0.09 to 0.2 cm year^{−1}, and typical grain size phi (Φ) of ~8.1 to 8.5 (14–16). Overlying water in central GPB has a seasonal temperature range of ~0 to 27°C and is well oxygenated throughout the year with salinities ranging from ~26 to 31. The benthic community is characterized by an upper bioturbated tier populated by the highly active deposit-feeding ophiuroid *Amphioplus abida*, which intensely reworks sediment as evidenced by penetration of the particle-associated, natural radionuclide ⁷Be [half-life (*t*_{1/2}) = 53 days] to depths of ~12 to 14 cm (fig. S1). Tube-building infauna includes the deposit-feeding maldanid polychaete *Sabaco elongata* and the suspension-feeding chaetopterid polychaete *Chaetopterus variopedatus*. These species

School of Marine and Atmospheric Sciences, Stony Brook University, Stony Brook, NY 11794, USA.

*Corresponding author. Email: robert.aller@stonybrook.edu

†Present address: NOAA, Global Monitoring Division, Boulder, CO 80305, USA.

typically build stable “parchment”-lined tubes encrusted with 2- to 3-mm agglutinated mud that extend ~20 to 25 cm [\sim 2 mm inside diameter (ID)] and 20 to 40 cm (\sim 20 mm ID), respectively, depending on the size of individuals (Fig. 1A and fig. S2). A deeper tier bioturbated zone dominated by the mantis shrimp *Squilla empusa* extends to \sim 2 to 3 m (burrows, \sim 5 cm ID) (16).

Additional cores containing *Chaetopterus* were obtained from muds in Smithtown Bay, Long Island Sound (LIS), USA (2005) and from site P in central LIS (2008 and 2010). These well-oxygenated sites have similar depths (\sim 14 to 15 m), water column salinities (\sim 27), bioturbation intensities, and sediment properties to the central GPB site (17, 18). LIS samples were used to examine fine-scale compositional gradients radially around *Chaetopterus* tubes and within tube linings, including pH, Fe and Mn, and authigenic minerals.

Sediment sampling

Solute and bacteria distribution patterns within the upper 25 cm of the GPB site were measured at different seasons in multiple box cores across two-dimensional (2D) (planar) sections oriented both vertically and horizontally. Solute exchange with overlying water and transport internally in the deposit were quantified by introduction of the conservative tracer NaBr (5 to 10 mM; seawater background, \sim 0.75 mM) to overlying water within 1 to 2 days after core collection (19). Spacing of sampling ports was centered at 2-cm grid points in arrays horizontally or vertically across the sides or tops of cores (fig. S3). Rhizon pore water extractors extended 3 to 5 cm into cores perpendicular to the array planes. Approximately 105 to 150 samples were obtained per core. Pore water samples were analyzed for Br^- , alkalinity, nutrients, Mn^{2+} , and Fe^{2+} (Materials and Methods). Only a subset of results is reported here and specifically from box cores containing inhabited *Chaetopterus* tubes.

Additional samples from GPB were used to examine fine-scale compositional gradients radially around *Chaetopterus* tubes, as well as in cores lacking *Chaetopterus*. Analyses included counts of bacteria (free cells and filaments), concentrations of total solid chromium reducible S (CRS \sim S^0 , FeS, FeS_2), and measurements of pore water Fe^{2+} and H_2S .

Bacteria and compositional patterns

Radial sampling around individual *Chaetopterus* tubes (July 2016, October 2016, and July 2018) demonstrated the direct association of cable bacteria with tube linings. The longest filaments (\sim 400 μm) were found closest to tube walls (Fig. 1 and fig. S4). Filament lengths decreased within the first few millimeters radially away from tube linings; however, average filament lengths and maximum observed lengths were generally enhanced within a few centimeters near tubes (1 to 3 cm) relative to more distal regions.

Br^- tracer penetrated in heterogeneous patterns to the base of box cores within 20 to 24 hours and showed domains of high and low concentrations at depth clearly related to biogenic structure (Fig. 2A). Pore water Cl^- concentrations were homogeneous within analytical error (\pm 1%). Br^- was preferentially transported around irrigated structures, including aggregations of *Sabaco* tubes or *Amphioplus*, but Br^- distributions were dominated by *Chaetopterus* tubes, the organic linings of which are diffusively permeable to low-molecular weight solutes such as O_2 and Br^- but impermeable to fluid advection (20). *Chaetopterus* tubes were surrounded by oxidized sediment (light yellow; orange in color), an additional indicator of habitation and active, sustained irrigation with oxygenated overlying water. Regions of low Br^- were also characterized by elevated alkalinity (\sim HCO_3^-) and NH_4^+ , both products of anaerobic metabolism, relative to regions of high Br^- (Fig. 2B and fig. S5A).

Cable bacteria filaments and free bacterial cells were abundant in subsurface aggregations associated with regions of high Br^- concentrations and specifically *Chaetopterus* tubes (Fig. 2, C and D). Relatively longer cables were present in the vicinity of tubes, ranging to $>$ 400 μm in Fig. 2 examples. No centimeter-long filaments were observed in any samples.

Horizontal sections within box cores demonstrated that cable bacteria filaments were ubiquitously present. Disseminated filaments were generally very short, however, often composed of 5 to 15 cells, except in the vicinity of *Chaetopterus* tubes, where, as in radial samples, lengths increased substantially. In the horizontal array section, filaments reached at least 650 μm as a tube was approached (Fig. 3). Examination

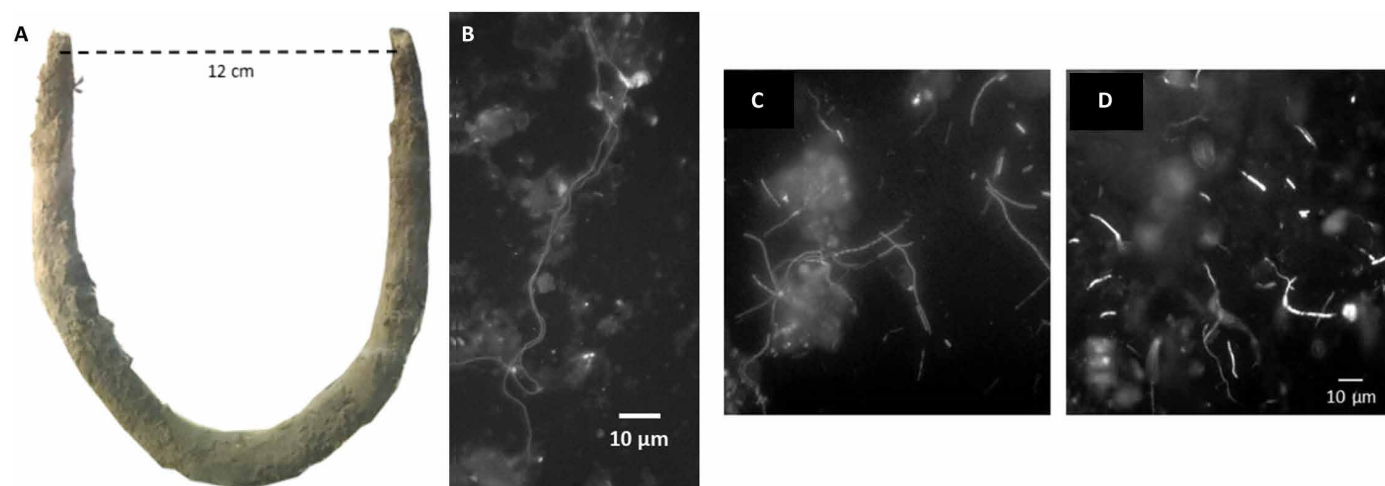


Fig. 1. Example *Chaetopterus* tube and tube-associated cable bacteria. (A) Example *Chaetopterus* tube (small), with agglutinated mud layer exhumed from box core and suspended in seawater (GPB; May 2018). Dotted scale line is located along sediment-water interface. (B) Cable bacteria filament in 1-mm layer scrapped from a tube lining (GPB; July 2017). Length, \sim 350 μm . (C) Cable bacteria filaments in agglutinated mud layer, 2- to 3-mm-thick annulus surrounding a tube lining [adjacent to (B)]; scale as in (D)]. Mean length, $20 \pm 9 \mu\text{m}$ (SD); minimum, 5 μm ; maximum, 80 μm . (D) Filaments in radial zone 3 to 5 mm surrounding a tube lining [adjacent to (C)]. Mean length, $11 \pm 8 \mu\text{m}$ (SD); minimum, 5 μm ; maximum, 40 μm .

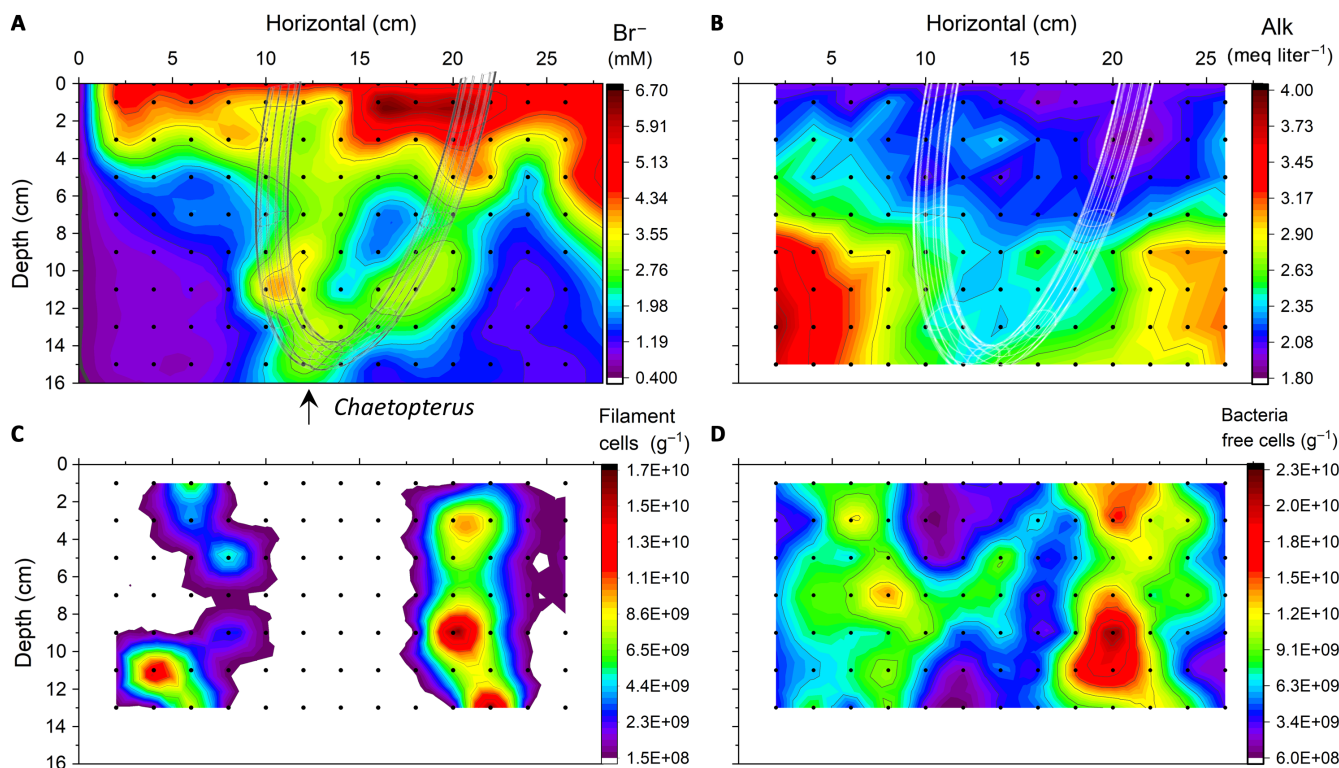


Fig. 2. 2D vertical Br^- tracer penetration, alkalinity, and bacterial distributions. (A) Br^- tracer penetration pattern in 2D vertical plane (5 cm thick perpendicular to section) after ~20 hours (GPB; June 2016; sediment-water interface at depth 0). A schematic net outlines approximate position of an inhabited U-shaped *Chaetopterus* tube located along the inner boundary of the sampled sediment section (~5 to 6 cm from the core face; right arm angled slightly into the core). Dots indicate locations of pore water samples. (B) Pore water alkalinity distribution in box core. (C) Cable bacteria filament cell counts (white indicates below detection for sample size). (D) Free bacteria cell counts corresponding to sub-array of (A). Both cable filament cells and free cells have elevated abundance near *Chaetopterus* tube sections and subdomains of enhanced solute exchange with overlying oxygenated water.

of additional box cores from GPB without *Chaetopterus* tubes revealed that low counts of short cable filaments either characterize the horizontal array sections distal to tubes (Fig. 3C) or were below detection as illustrated in Fig. 2C.

Geochemical evidence of cable bacteria activity associated with *Chaetopterus* tubes consists of elevated pH adjacent to the oxic lining, solid-phase S gradients with depletion around the tube ($\text{CRS} \sim \text{S}^0$, FeS, FeS₂), and focused authigenic mineral precipitates within the tube lining (cathodic terminus) usually composed predominantly of Mn-oxides but sometimes Fe-oxides (Figs. 4, A and B, and 5B). Energy dispersive spectroscopy (EDS) analyses demonstrated that the relative concentrations of Mn and Fe can vary along tubes, although Mn is generally dominant. Reactive Fe and Mn leaches of tube linings and ambient sediment from central LIS [station P (18)] showed Fe/Al and Mn/Al in linings averaging 14.6 ± 2.9 and $6.0 \pm 1.4 \mu\text{g g}^{-1}$ ($n = 5$), respectively, compared to sediment ratios of 1.38 ± 0.16 and 0.045 ± 0.008 ($n = 9$), indicating bulk tube/sediment Fe and Mn enrichments of ~11× and ~130×, respectively. Metal precipitates are not present in the tube material secreted by *Chaetopterus* in laboratory aquaria in the absence of surrounding sediment (Fig. 5A). The elevation of dissolved Fe²⁺ around tubes is also consistent with cable bacteria activity (Fig. 4D) (21, 22). Dissolved H₂S in these deposits is generally below 20 μM and is further depleted near all irrigated structures, including *Chaetopterus* (23). As in the case of other stable tube and burrows, the abundance of nematodes is enhanced at depth in the vicinity of *Chaetopterus* tubes (fig. S5) (24).

DISCUSSION

Br^- tracer tracks exchange of pore water with overlying water through the walls of ventilated dwellings and feeding cavities into surrounding sediment. Cable bacteria filaments and free bacterial cells were abundant in subsurface aggregations associated with regions of rapid solute exchange (Br^-) and specifically *Chaetopterus* tubes, which can be stable for months or more (Figs. 1 to 3). Relatively longer cables were present in the immediate vicinity of tubes, ranging to >650 μm in these examples (Figs. 1 to 3). The appearance times of filament aggregations near the sediment-water interface in laboratory microcosm incubations are ~7 to 10 days (11, 21, 25), suggesting that if transport conditions around subsurface biogenic structures are established for similar time scales, cable bacteria can and do respond. The occurrence of cable bacteria in close association with oxygenated regions of seagrass roots is consistent with this inference (26).

We have never directly observed filaments of centimeter length in natural sediments, perhaps as a result of fragmentation during separation for identification and counting, despite geochemical indicators (pH distributions) that would suggest these scales (Fig. 4B). We note that with some exceptions (22, 27), most investigators report cable abundances that must also reflect typical lengths less than 1 to 5 mm, or major biases in sampling procedures that prevent accurate length measurements (4, 11, 22). If lengths of 1 to 5 mm or fewer cells are indeed common, electron conduction through networks of filaments and minerals rather than continuous cables may occur, or cells may optionally use local redox reaction pathways in a

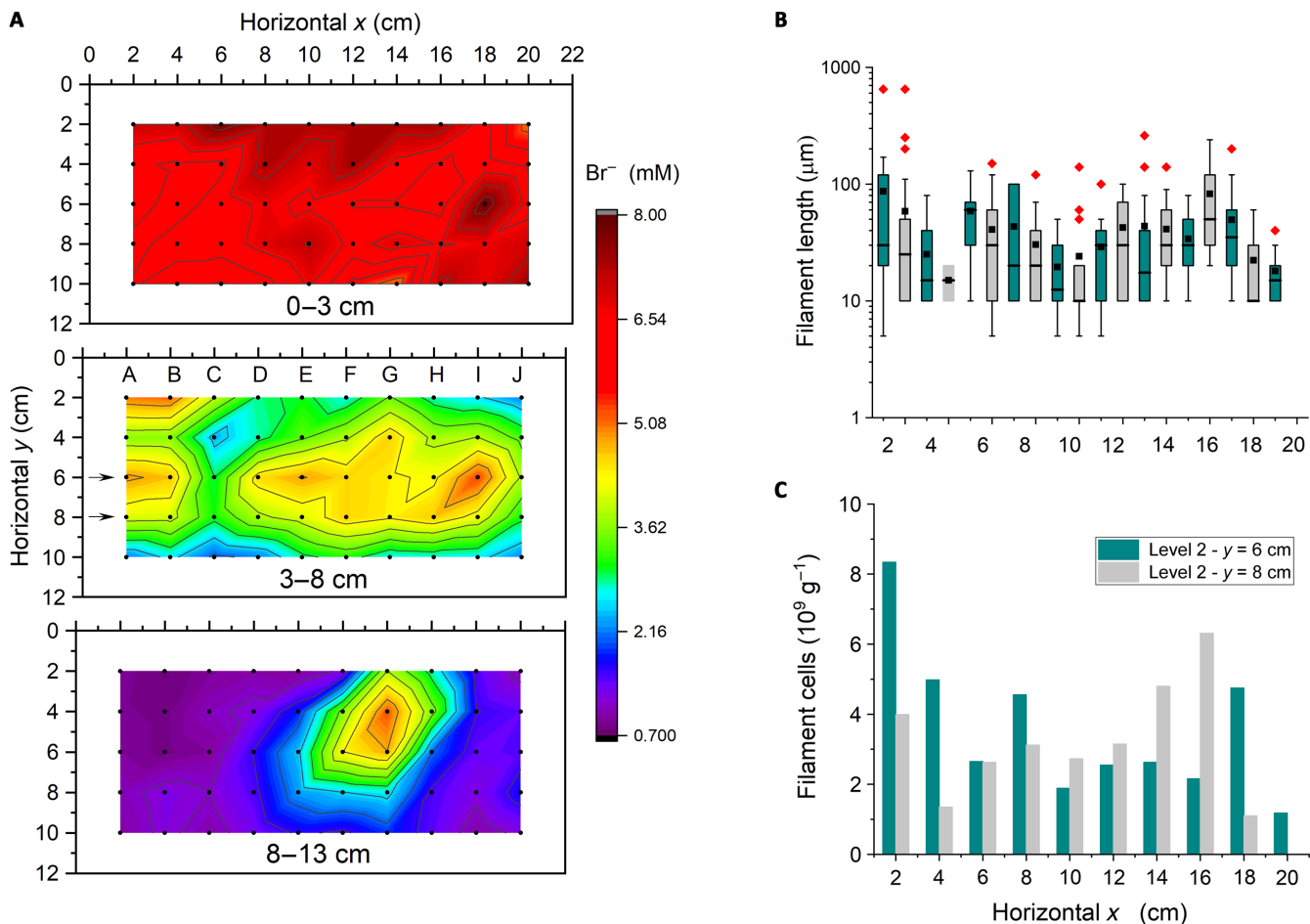


Fig. 3. 2D horizontal Br⁻ tracer and cable bacteria distributions. (A) Stacked horizontal sections (3 to 5 cm thick) showing Br⁻ penetration as a function of depth and horizontal planes. High penetration regions are associated primarily with two inhabited *Chaetopterus* tube sections (July 2017). (B) Box-whisker diagrams showing lengths of cable filaments at varying horizontal x positions separated along two transects within the 3- to 8-cm, level 2 interval (y = 6 and 8 cm; arrows). Black square, mean; line, median; red diamonds, outliers; box, 25 to 75% quartiles. (C) Filament cell abundance corresponding to array positions along transects (3- to 8-cm depth interval). Filaments occur through the sediment but with the longest filaments and most abundant filament cells found closest to regions of greatest Br⁻ concentrations near *Chaetopterus* tubes.

traditional mode. In any case, we presume that the relative distributions are accurate and imply more optimal growth of cables in association with *Chaetopterus* tubes.

Geochemical evidence of cable bacterial activity associated with *Chaetopterus* tubes consists of elevated pH at the oxygenated wall and a distal pH minimum, solid-phase S gradients with depletion around tubes, and focused authigenic mineral precipitates within the tube lining (cathodic terminus), in these cases composed predominantly of Mn and Fe oxides (Fig. 5B). The scaling of the elevated pH zone relative to the pH minimum presumably reflects the radial symmetry and volumetrically comparable anodic and cathodic zones (e.g., annulus areas defined by radius distance differences, expand as a function of radius) (Fig. 4B). Mn, in particular, is strongly enriched at the oxygenated tube boundary relative to surrounding sediment (>130×). Oxidic and anoxic incubations of tube material suggest that the Mn-oxide micronodules inhibit aerobic decomposition of the carbohydrate-rich tube linings (28). The elevation of dissolved Fe²⁺ around tubes is also consistent with cable bacteria activity and Fe-oxide enrichment in the tube lining (Fig. 4D). Dissolved H₂S in these deposits is generally below 20 μM and

is further depleted near all irrigated structures, including *Chaetopterus* (23). Although, with the exception of elevated pH at the inner tube wall, the geochemical patterns need not be uniquely due to cable bacteria, they are consistent with reactions associated with the activity of cable bacteria, which, along with associated consortia of S oxidizers and reducers (11, 12), presumably promotes them. The overall relationships imply a mutualistic association between macro- and microfauna, with the former benefiting from enhanced tube longevity, lowered sulfide fluxes, and scavenging of potential toxins by Mn, Fe-oxide precipitates, and the latter by stable physical conditions and a reliably oxidized interface. As in the case of other stable tube and burrows, the abundance of nematodes is generally enhanced near *Chaetopterus* tubes, and they may be important in grazing the elevated populations of both cable and free bacteria (fig. S5) (24).

CONCLUSIONS

These data demonstrate that cable bacteria can be abundant in intensely bioturbated deposits, particularly in aggregations directly

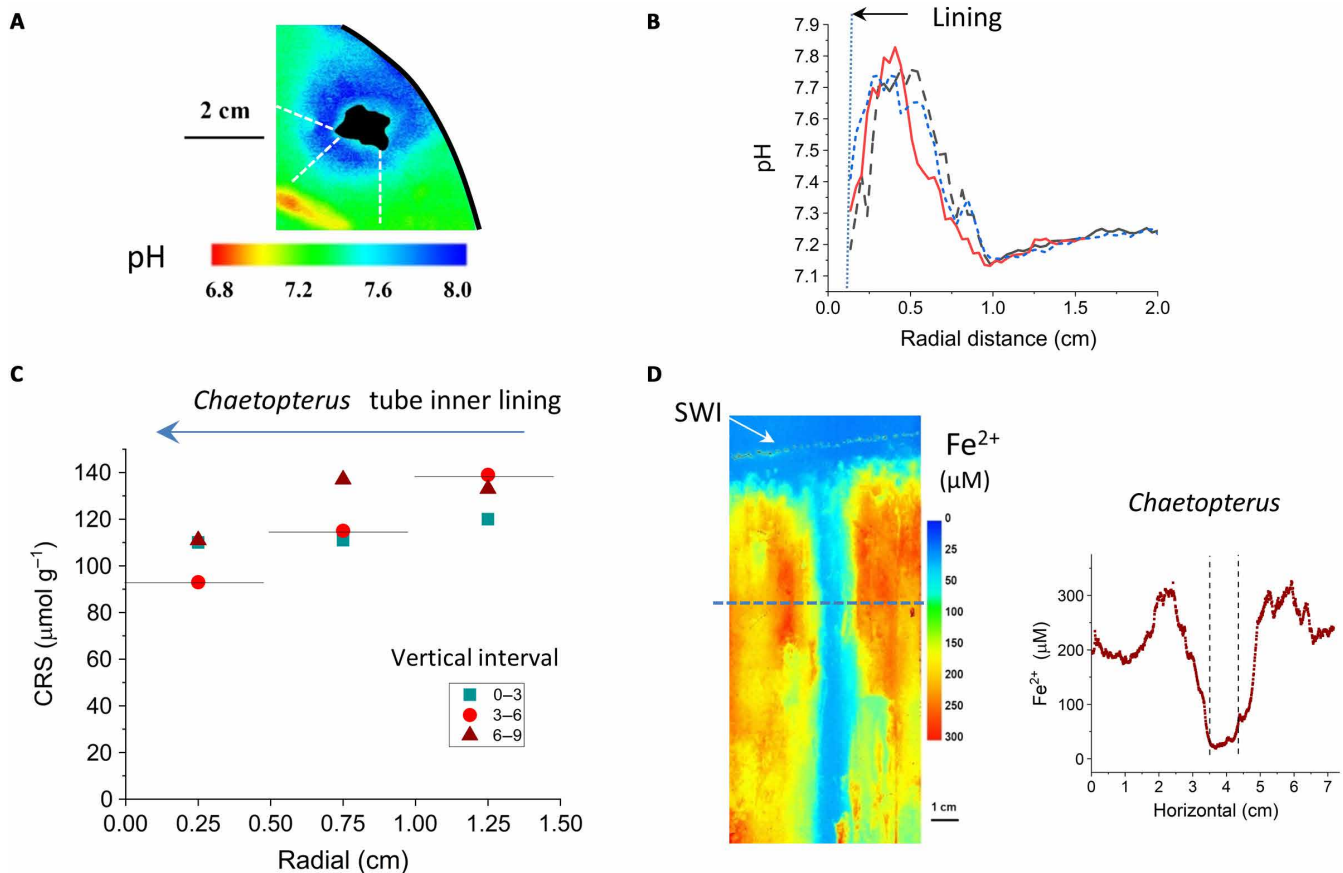


Fig. 4. pH, sediment S, and dissolved Fe^{2+} distributions around *Chaetopterus* tubes. (A) 2D radial pH distribution around *Chaetopterus* tube revealed in horizontal section of a core by planar pH optode, demonstrating elevated pH associated with tube lining and immediately surrounding sediment (LIS Smithtown Bay site). The low pH trail (bottom left) is the body surface of a polychaete, *Nephtys incisa*, moving horizontally within the sampling plane. The water level in the oxygenated tube lumen was below the pH sensor film during imaging and is shown as black. The curved core liner boundary is also shown as black. The white dotted lines represent locations of radial pH transects beginning at the tube lining boundary. (B) Radial transects of pH derived from (A). The radial geometry enhances the apparent elevated pH zone extent relative to the pH minimum zone (i.e., annulus areas defined by radius distance differences, change as a function of radius). (C) Radial transects of CRS around *Chaetopterus* tube showing depletion of solid-phase S toward tube within all vertical depth intervals (0 to 3, 3 to 6, and 6 to 9 cm). Bars indicate radial annulus of sample. (D) 2D dissolved Fe^{2+} distribution around *Chaetopterus* tube from GPB site. SWI, sediment-water interface. A radial distribution of Fe^{2+} at a depth of ~5 cm (horizontal dotted line on image) illustrates enhanced concentrations at distances of 1 to 2 cm from the tube wall (vertical dotted lines) and concentration gradients toward the lining that result in Fe-oxide deposition.

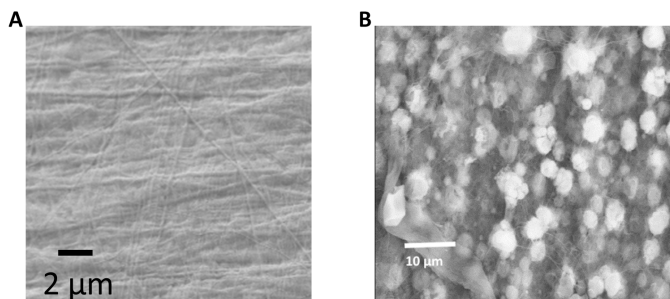


Fig. 5. *Chaetopterus* tube lining formed in seawater or within sediment. (A) SEM image of tube lining formed by *Chaetopterus* in a laboratory aquarium in the absence of sediment. No authigenic mineral precipitates are evident. The $\sim 60^\circ \times 120^\circ$ oriented polymer strand structure is common in polychaete tube linings (20). (B) *Chaetopterus* tube linings formed in situ are permeated with micromodules of Mn oxide, often preferentially aligned with polymer strands. Fe oxide-rich precipitates are also present and can dominate in some sections of linings; however, Mn enrichment is more common (SEM; scale bar, 10 μm).

associated with physically stable and irrigated biogenic structures, in this case, predominantly *Chaetopterus* tubes. The presence of short filament sections throughout the bioturbated zone in the sulfidic estuarine muds of GPB, together with the demonstration of metabolic flexibility (9, 10), implies that these organisms are opportunistic and facultative and are capable of responding to the presence of stable (about >1 week), oxygenated microenvironments generated by macrofauna and to a range of biogeochemical conditions. These distribution patterns further imply that the present dominant description of cable bacteria likely represents an end-member life habit and morphological expression in a continuum: from classic metabolic adaptations associated with local redox conditions and traditional successional zonation to conducting filaments promoting nonlocal electron transport in physically stable, 2D and 3D electrogenic grids. We conclude that the evolution of bioturbation and biogenic structure in the late Proterozoic and early Phanerozoic (~550 million years ago) (29) did not substantially inhibit cable bacteria but rather further enhanced their ecological options.

MATERIALS AND METHODS**Sampling**

During core handling and tracer penetration periods, box cores were immersed in seawater in the laboratory at in situ collection temperatures (15° to 22°C), and the water overlying cores was continuously aerated to maintain O₂ saturation. At ~20 to 24 hours following tracer introduction, overlying water was removed and, for vertically oriented sections, the core sides were gently replaced with thin (2 mm) plastic sheets, with holes drilled in 2D grids to receive Rhizon pore water extractors (2 mm diameter, 5 cm length, 0.2 μm pore size; Rhizosphere Research Products). Horizontal arrays were similarly obtained using drilled plastic sheet for orientation at successive depth levels.

Pore water

Extracted pore water (2 to 3 ml) and overlying water samples were divided into two portions: one left unacidified and used for Br⁻, Cl⁻, alkalinity, and NH₄⁺ analyses, and one acidified to 0.1N with HCl and analyzed for dissolved inorganic phosphate (DIP ~HPO₄²⁻), NO₃⁻, Mn²⁺, Si(OH)₄, Mn²⁺, and Fe²⁺ as permitted by total sample sizes. A subset of Br⁻, Cl⁻, alkalinity, and NH₄⁺ data is reported here. Cl⁻ (total halides corrected for Br⁻) was measured in triplicate on 20-μl samples using a potentiometric titration with Ag⁺ (precision, 1%; Radiometer CMT10); Br⁻ was measured in triplicate on 25-μl samples using a 96-well plate modification of the phenol red–bromophenol blue method (precisions, 2 to 5%) (30); alkalinity was measured in triplicate on 100-μl samples using a 96-well plate modification of the formic acid–bromophenol blue method (precisions, 3 to 5%) (31).

Sediment

All box cores were subsampled for sediment water content and porosity estimates using cutoff 60-ml syringes extruded over 1-cm vertical depth intervals. Sediment was weighed wet and dry (70°C). Porosity was estimated from water content assuming a particle density of 2.6 g cm⁻³.

Reactive Fe, Mn, and Al were estimated by leaching tube linings or sediment with 1 N HCl for 16 hours at 22°C. Fe and Mn were measured spectrophotometrically using ferrozine and formaldoxime (32, 33) and Al using graphite furnace atomic absorption. Solid-phase S was measured as CRS at 22°C using passive distillation (34).

Sediment samples for direct epifluorescence counts of free-living bacteria cell and cable bacteria distributions were obtained using cutoff 3-ml plastic syringes inserted at the same locations as Rhizon ports and immediately preserved with 2% formaldehyde in sterile seawater (3% salt) and refrigerated. Sample syringes sometimes intersected tubes but did not pierce the tough lining material. These samples were used to enumerate total free-living bacteria cells and cable bacteria, the latter identifiable by the unmistakable filament morphology, after staining with acridine orange (AO) (35, 36). Confirmation of cable bacteria identity was made on subsamples at all array locations, and radial intervals by fluorescence in situ hybridization (FISH) with a Desulfobulbaceae-specific oligonucleotide probe (DSB706; 5'-ACCCGATTCCTCCCGAT-3') (37), EUB338 probe mixture (38), and probe NON338 (39) were used as positive and negative controls, respectively, with FISH protocols according to (40) and probe hybridization conditions after (25). The length of filaments and number of cells were made from the AO-stained samples, which not only were larger than the FISH confirmation samples but also were minimally disturbed as opposed to the smaller subsamples

used for FISH. AO-stained black 0.2-μm neutron track-etched polycarbonate membrane filters with 100-fold diluted samples of sediment for direct counts of bacteria by epifluorescence microscopy after (35) (precision better than 5.0%). Free-living cells within 10 randomly selected fields defined by a Whipple reticle (0.1 mm by 0.1 mm) of 100 0.01 mm by 0.01 mm squares were counted, while cable cells were counted or filament lengths (including any that extended beyond the grid field) recorded within at least 20 fields systematically covering the filter. The number of individual cable cells per filament of a given length was calculated on the basis of repeated measurements of five cells across a reticle grid square. After removal of subsamples for bacterial counts and wet-dry weight conversion, the remaining sediment was stained with rose bengal, allowed to sit for several hours to overnight, collected on a 0.44-μm nylon-mesh screen, and rinsed with distilled water, and nematodes were enumerated under a dissecting microscope.

For radiochemical analyses (⁷Be), sediment cores (9.5 cm ID) were obtained at multiple times in 2009–2010 and 2018 at the sampling site using 10-cm outside diameter cellulose acetate butyrate (CAB) corer tubes as subcorers of larger box cores obtained by divers. These cylindrical cores were sectioned at 1- to 3-cm intervals, dried, ground, and γ-counted for ⁷Be (477 keV; Canberra 3 K LeGe). Counting error was used as a measure of analytical precision. Example profiles from July to October 2009 and September 2018 are reported here. These sampling periods are from the same seasons as box cores obtained for analyses of cable bacteria.

In the case of radial sampling, tubes from both sampling sites were also removed from sediment and cleaned of agglutinated mud by scrapping and sonification in seawater followed by a single rinse with distilled water to remove salt, and the microstructure was examined by scanning electron microscopy (SEM)/EDS. A cylindrical core containing a *Chaetopterus* tube collected from Smithtown Bay, LIS, USA (17) was sectioned horizontally during extrusion, and pH distributions were measured in horizontal planes radially around the tube at multiple depths.

2D pH distributions were measured using reversible planar optodes either placed horizontally directly onto sectioned core surfaces or inserted vertically along the sides of box corers (41).

Dissolved Fe²⁺ and H₂S (as dissolved H₂S only) distributions were measured using irreversible planar sensors inserted vertically into sediment cores next to *Chaetopterus* tubes and/or allowed to equilibrate for 3 to 5 min (23, 42). X-radiography of sedimentary structure was performed on 2.5-cm-thick vertical subcores of box cores or separate diver-taken box cores 2.5 cm in thickness using a Kramex portable x-ray source (80 kilovolt peak, 10 mA; 0.04 s) and a Samsung LTX 1717 digital x-ray detector.

SUPPLEMENTARY MATERIALS

Supplementary material for this article is available at <http://advances.sciencemag.org/cgi/content/full/5/7/eaaw3651/DC1>

Authors note

Fig. S1. Representative ⁷Be profiles.

Fig. S2. X-radiographs of *Chaetopterus* tube and sedimentary structure.

Fig. S3. Schematic diagram of Rhizon sampling array orientations.

Fig. S4. Example FISH confirmation of cable bacteria and filament length.

Fig. S5. 2D NH₄⁺ and nematode abundance patterns.

REFERENCES AND NOTES

1. L. P. Nielsen, N. Risgaard-Petersen, H. Fossing, P. B. Christensen, M. Sayama, Electric currents couple spatially separated biogeochemical processes in marine sediment. *Nature* **463**, 1071–1074 (2010).

2. L. P. Nielsen, N. Risgaard-Petersen, Rethinking sediment biogeochemistry after the discovery of electric currents. *Ann. Rev. Mar. Sci.* **7**, 425–442 (2015).
3. S. Y. Malkin, A. M. F. Rao, D. Seitaj, D. Vasquez-Cardenas, E.-M. Zetsche, S. Hidalgo-Martinez, H. T. S. Boschker, F. J. R. Meysman, Natural occurrence of microbial Sulphur oxidation by long-range electron transport in the seafloor. *ISME J.* **8**, 1843–1854 (2014).
4. S. Y. Malkin, D. Seitaj, L. D. W. Burdorf, S. Nieuwhof, S. Hidalgo-Martinez, A. Trampler, N. Geeraert, H. De Stigter, F. J. R. Meysman, Electrogenic sulfur oxidation by cable bacteria in bivalve reef sediments. *Front. Mar. Sci.* **4**, 28 (2017).
5. D. Seitaj, R. Schauer, F. Sulu-Gambari, S. Hidalgo-Martinez, S. Y. Malkin, L. D. W. Burdorf, C. P. Slomp, F. J. R. Meysman, Cable bacteria generate a firewall against euxinia in seasonally hypoxic basins. *Proc. Natl. Acad. Sci. U.S.A.* **112**, 13278–13283 (2015).
6. L. D. W. Burdorf, A. Trampler, D. Seitaj, L. Meire, S. Hidalgo-Martinez, E.-M. Zetsche, H. T. S. Boschker, F. J. R. Meysman, Long-distance electron transport occurs globally in marine sediments. *Biogeochem.* **14**, 683–701 (2017).
7. F. J. R. Meysman, N. Risgaard-Petersen, S. Y. Malkin, L. P. Nielsen, The geochemical fingerprint of microbial long-distance electron transport in the seafloor. *Geochim. Cosmochim. Acta* **152**, 122–142 (2015).
8. F. Sulu-Gambari, D. Seitaj, T. Behrends, D. Banerjee, F. J. R. Meysman, C. P. Slomp, Impact of cable bacteria on sedimentary iron and manganese dynamics in a seasonally-hypoxic marine basin. *Geochim. Cosmochim. Acta* **192**, 49–69 (2016).
9. U. Marzocchi, D. Trojan, S. Larsen, R. L. Meyer, N. P. Revsbech, A. Schramm, L. P. Nielsen, N. Risgaard-Petersen, Electric coupling between distant nitrate reduction and sulfide oxidation in marine sediment. *ISME J.* **8**, 1682–1690 (2014).
10. C. E. Reimers, C. Li, M. F. Graw, P. S. Schrader, M. Wolf, The identification of cable bacteria attached to the anode of a benthic microbial fuel cell: Evidence of long distance extracellular electron transport to electrodes. *Front. Microbiol.* **8**, 2055 (2017).
11. D. Vasquez-Cardenas, J. van de Vossen, L. Polerecky, S. Y. Malkin, R. Schauer, S. Hidalgo-Martinez, V. Confurius, J. J. Middelburg, F. J. R. Meysman, H. T. S. Boschker, Microbial carbon metabolism associated with electrogenic sulphur oxidation in coastal sediments. *ISME J.* **9**, 1966–1978 (2015).
12. D. R. Lovley, Happy together: Microbial communities that hook up to swap electrons. *ISME J.* **11**, 327–336 (2017).
13. D. Trojan, L. Schreiber, J. T. Bjerg, A. Bøggild, T. Yang, K. U. Kjeldsen, A. Schramm, A taxonomic framework for cable bacteria and proposal of the candidate genera *Electrothrix* and *Electronema*. *Syst. Appl. Microbiol.* **39**, 297–306 (2016).
14. J. K. Cochran, D. Hirschberg, D. Amiel, "Particle mixing and sediment accumulation rates of Peconic Estuary sediments: A sediment accretion study in support of the Peconic Estuary Program" (Final Report of Project #0014400498181563, Marine Sciences Research Center, Stony Brook Univ., (2000).
15. R. Cerrato, R. Flood, L. Holt, "Mapping for habitat classification in the Peconic Estuary: Phase III ground truth studies" (Special Report #137, Suffolk County Department of Health Services, Marine Science Research Center, Stony Brook Univ., 2010).
16. S. Waugh, R. C. Aller, N₂ production and fixation in deep-tier burrows of *Squilla empusa* in muddy sediments of Great Peconic Bay. *J. Sea Res.* **129**, 36–41 (2017).
17. E. Michaud, R. C. Aller, G. Stora, Sedimentary organic matter distributions, burrowing activity, and biogeochemical cycling: Natural patterns and experimental artifacts. *Estuar. Coast. Shelf Sci.* **90**, 21–34 (2010).
18. M. Gerino, R. C. Aller, C. Lee, J. K. Cochran, J. Y. Aller, M. A. Green, D. Hirschberg, Comparison of different tracers and methods used to quantify bioturbation during a spring bloom: 234-Thorium, luminophores and chlorophylla. *Estuar. Coast. Shelf Sci.* **46**, 531–547 (1998).
19. W. R. Martin, G. T. Banta, The measurement of sediment irrigation rates: A comparison of the Br⁻ tracer and ²²²Rn/²²⁶Ra disequilibrium techniques. *J. Mar. Res.* **50**, 125–154 (1992).
20. R. C. Aller, The importance of the diffusive permeability of animal burrow linings in determining marine sediment chemistry. *J. Mar. Res.* **41**, 299–322 (1983).
21. A. M. F. Rao, S. Y. Malkin, S. Hidalgo-Martinez, F. J. R. Meysman, The impact of electrogenic sulfide oxidation on elemental cycling and solute fluxes in coastal sediment. *Geochim. Cosmochim. Acta* **172**, 265–286 (2016).
22. S. van de Velde, L. Lesven, L. D. W. Burdorf, S. Hidalgo-Martinez, J. S. Geelhoed, P. Van Rijswijk, Y. Gao, F. J. R. Meysman, The impact of electrogenic sulfur oxidation on the biogeochemistry of coastal sediments: A field study. *Geochim. Cosmochim. Acta* **194**, 211–232 (2016).
23. H. Yin, Q. Zhu, R. C. Aller, An irreversible planar optical sensor for multi-dimensional measurements of sedimentary H₂S. *Mar. Chem.* **195**, 143–152 (2017).
24. J. Y. Aller, R. C. Aller, Evidence for localized enhancement of biological associated with tube and burrow structures in deep-sea sediments at the HEEBLE site, western North Atlantic. *Deep Sea Res. Part 1 Oceanogr. Res. Pap.* **33**, 755–790 (1986).
25. R. Schauer, N. Risgaard-Petersen, K. U. Kjeldsen, J. J. T. Bjerg, B. B. Jørgensen, A. Schramm, L. P. Nielsen, Succession of cable bacteria and electric currents in marine sediment. *ISME J.* **8**, 1314–1322 (2014).
26. B. C. Martin, J. Bougoure, M. H. Ryan, W. W. Bennett, T. D. Colmer, N. K. Joyce, Y. S. Olsen, G. A. Kendrick, Oxygen loss from seagrass roots coincides with colonisation of sulphide-oxidising cable bacteria and reduces sulphide stress. *ISME J.* **13**, 707–719 (2019).
27. R. Cornillisen, A. Bøggild, R. Thiruvallur Eachambadi, R. I. Koning, A. Kremer, S. Hidalgo-Martinez, E.-M. Zetsche, L. R. Damgaard, R. Bonn , J. Drijkoningen, J. S. Geelhoed, T. Boesen, H. T. S. Boschker, R. Valcke, L. P. Nielsen, J. D'Haen, J. V. Manca, F. J. R. Meysman, The cell envelope structure of cable bacteria. *Front. Microbiol.* **9**, article 3044 (2018).
28. A. Kaushik, "Diagenetic behavior of structural materials formed by benthic macrofauna," thesis, Stony Brook University, Stony Brook, NY (2011).
29. M. G. Mngano, L. A. Buatois, The Cambrian explosion, in *The Trace Fossil Record of Major Evolutionary Events, Volume 1. Precambrian and Paleozoic. Topics in Geobiology, M. G. Mngano, L. A. Buatois, Eds.* (Springer, 2016), vol. 39, pp. 73–126.
30. B. J. Lepore, P. A. Barak, A colorimetric microwell method for determining bromide concentrations. *Soil Sci. Soc. Am. J.* **73**, 1130–1136 (2009).
31. G. Sarazin, G. Michard, F. A. Prevot, A rapid and accurate spectroscopic method for alkalinity measurements in sea water samples. *Water Res.* **33**, 290–294 (1999).
32. L. L. Stookey, Ferrozine—A new spectrophotometric reagent for iron. *Anal. Chem.* **42**, 779–781 (1970).
33. K. Goto, T. Komatsu, T. Furukawa, Rapid colorimetric determination of manganese in waters containing iron: A modification of the formaldoxime method. *Anal. Chim. Acta* **27**, 331–334 (1962).
34. H. Fossing, B. B. Jørgensen, Measurement of bacterial sulfate reduction in sediments: Evaluation of a single-step chromium reduction method. *Biogeochem.* **8**, 205–222 (1989).
35. J. E. Hobbie, R. J. Daley, S. Jasper, Use of nucleopore filters for counting bacteria by fluorescence microscopy. *Appl. Environ. Microbiol.* **33**, 1225–1228 (1977).
36. S. W. Watson, T. J. Novitsky, H. L. Quinby, F. W. Valois, Determination of bacterial number and biomass in the marine environment. *Appl. Environ. Microbiol.* **33**, 940–946 (1977).
37. W. Manz, R. Amann, W. Ludwig, M. Wagner, K. H. Schleifer, Phylogenetic oligodeoxynucleotide probes for the major subclasses of proteobacteria: Problems and solutions. *Syst. Appl. Microbiol.* **15**, 593–600 (1992).
38. R. I. Amann, B. J. Binder, R. J. Olson, S. W. Chisholm, R. Devereux, D. A. Stahl, Combination of 16S rRNA-targeted oligonucleotide probes with flow cytometry for analyzing mixed microbial populations. *Appl. Environ. Microbiol.* **56**, 1919–1925 (1990).
39. G. Wallner, R. Amann, W. Beisker, Optimizing fluorescent in situ hybridization with rRNA-targeted oligonucleotide probes for flow cytometric identification of microorganisms. *Cytometry* **14**, 136–143 (1993).
40. J. Perntaler, F.-O. Glöckner, W. Schönhuber, R. Amann, Fluorescence in situ hybridization (FISH) with rRNA-targeted oligonucleotide probes. *Methods Microbiol.* **30**, 207–210 (2001).
41. Q. Z. Zhu, R. C. Aller, Y. Fan, Two-dimensional pH distributions and dynamics in bioturbated marine sediments. *Geochim. Cosmochim. Acta* **70**, 4933–4949 (2006).
42. Q. Zhu, R. C. Aller, Two-dimensional dissolved ferrous iron distributions in marine sediments as revealed by a novel planar optical sensor. *Mar. Chem.* **136-137**, 14–23 (2012).

Acknowledgments: We thank S. Waugh, H. Yin, W. Cong, B. Gagliardi, and A. Brosnan for assistance in the field; J. Quinn (SBU) for overseeing or carrying out SEM/EDS analyses; and C. Reimers and A. Rao for critical review comments. Excerpts of research were publicly presented at CERF 2017 and Goldschmidt 2018 conferences. **Funding:** Supported by NSF OCE 1737749 and NSF OCE 1332418. **Author contributions:** R.C.A.: project conception; R.C.A., C.H., I.K., A.K., and Q.Z.: field and laboratory sampling; J.Y.A.: microbial and meiofauna measurements; C.H., Q.Z., I.K., and A.K.: pore water, sensor, and sediment analyses; A.K. and R.C.A.: SEM/EDS analyses; R.C.A., J.Y.A., Q.Z., and C.H.: data interpretation and manuscript preparation. **Competing interests:** The authors declare that they have no competing interests. **Data and materials availability:** All data needed to evaluate the conclusions in the paper are present in the paper and/or the Supplementary Materials. Additional data related to this paper may be requested from the authors.

Submitted 12 December 2018

Accepted 14 June 2019

Published 17 July 2019

10.1126/sciadv.aaw3651

Citation: R. C. Aller, J. Y. Aller, Q. Zhu, C. Heilbrun, I. Klingensmith, A. Kaushik, Worm tubes as conduits for the electrogenic microbial grid in marine sediments. *Sci. Adv.* **5**, eaaw3651 (2019).

Worm tubes as conduits for the electrogenic microbial grid in marine sediments

Robert C. Aller, Josephine Y. Aller, Qingzhi Zhu, Christina Heilbrun, Isaac Klingensmith and Aleya Kaushik

Sci Adv 5 (7), eaaw3651.

DOI: 10.1126/sciadv.aaw3651

ARTICLE TOOLS

<http://advances.sciencemag.org/content/5/7/eaaw3651>

SUPPLEMENTARY MATERIALS

<http://advances.sciencemag.org/content/suppl/2019/07/15/5.7.eaaw3651.DC1>

REFERENCES

This article cites 38 articles, 4 of which you can access for free
<http://advances.sciencemag.org/content/5/7/eaaw3651#BIBL>

PERMISSIONS

<http://www.sciencemag.org/help/reprints-and-permissions>

Use of this article is subject to the [Terms of Service](#)

Science Advances (ISSN 2375-2548) is published by the American Association for the Advancement of Science, 1200 New York Avenue NW, Washington, DC 20005. The title *Science Advances* is a registered trademark of AAAS.

Copyright © 2019 The Authors, some rights reserved; exclusive licensee American Association for the Advancement of Science. No claim to original U.S. Government Works. Distributed under a Creative Commons Attribution NonCommercial License 4.0 (CC BY-NC).